Journal of Catalysis **196,** 73–85 (2000)
doi:10.1006/jcat.2000.3015, available online at http://www.idealibrary.com on IDEAL®

Catalytic Performance and Characterization of VO^{2+}-Exchanged Titania-Pillared Clays for Selective Catalytic Reduction of Nitric Oxide with Ammonia

R. Q. Long and R. T. Yang[1]

Department of Chemical Engineering, University of Michigan, Ann Arbor, Michigan 48109-2136

Received March 13, 2000; revised July 27, 2000; accepted July 31, 2000

VO^{2+} ion-exchanged TiO_2-pillared clays ($VO–TiO_2$-PILC) were investigated for selective catalytic reduction of nitric oxide by ammonia in the presence of oxygen. They were also characterized for surface area and pore size distribution and by X-ray diffraction (XRD), X-ray photoelectron spectroscopy (XPS), electron spin resonance (ESR), and Fourier transform infrared (FTIR) spectroscopy. It was found that $VO–TiO_2$-PILC catalysts were highly active for the selective catalytic reduction (SCR) reaction. The maximum activity was obtained with 2.1–3.5 wt% vanadium, which was close to or slightly higher than the activity of the commercial $V_2O_5 + WO_3/TiO_2$ catalyst. The $VO–TiO_2$-PILC catalysts were also resistant to water vapor and sulfur dioxide at high temperatures ($>350^\circ$C). XRD patterns of $VO–TiO_2$-PILC were similar to that of TiO_2-PILC, showing no peaks due to vanadium oxides, even when the vanadium content reached 13.2 wt%. XPS and ESR spectra indicated that vanadium was present mainly as the +5 valence form (probably as V_2O_5) on the fresh catalysts, but was partially reduced to the +4 form (VO^{2+}) after being heated at 300°C in He. The FTIR spectra of the adsorbed $NO + O_2$ suggested that vanadium oxides were anchored directly on the titania pillars of the catalysts. NH_3 molecules adsorbed on the Brønsted acid and Lewis acid sites to form, respectively, NH_4^+ ions and coordinated NH_3 species. These NH_3 adspecies were active in reaction with NO and $NO + O_2$. The Brønsted acidity increased with increasing vanadium content, which was consistent with an increase in the SCR activity for low temperatures (e.g., 200°C). By comparison, the adsorption of NO_x ($x = 1, 2$) on the catalysts was very weak, especially under reaction conditions. The present results indicate that the reaction path for NO reduction by NH_3 on $VO–TiO_2$-PILC is similar to that on V_2O_5/TiO_2; i.e., N_2 originates mainly from the reaction between gaseous or weakly adsorbed NO and NH_3 adspecies.

Key Words: **selective catalytic reduction; SCR of NO by NH_3; TiO_2-pillared clay; vanadyl-exchanged TiO_2-pillared clay; Brønsted acid site; Lewis acid site.**

INTRODUCTION

Selective catalytic reduction (SCR) of nitrogen oxides (NO_x, $x = 1, 2$) with ammonia is the most efficient technology for removing NO_x from power plants and other stationary sources. Many catalysts have been reported to be active for this reaction. A comprehensive review of SCR catalysts is available (1). The vanadia doped on supporters such as Al_2O_3, SiO_2, ZrO_2, TiO_2, and $TiO_2–SiO_2$ were studied extensively and $V_2O_5 + WO_3$ (or MoO_3) supported on TiO_2 has been commercialized due to its high activity and resistance to poisoning by H_2O and SO_2. The mechanism of the reaction on vanadia-based catalysts has been extensively studied and several different mechanisms have been proposed (1–10). Most researchers agree that the SCR reaction on vanadia catalysts follows an Eley–Rideal-type mechanism; i.e., a strongly adsorbed ammonia species reacts with a gaseous or weakly adsorbed NO molecule to form molecular N_2. However, which ammonia adspecies (Brønsted or Lewis) is involved in the reaction is still under debate (2). In addition to vanadia catalysts, other transition metal oxides (e.g., CuO, Fe_2O_3, Cr_2O_3, $Fe_2O_3–Cr_2O_3$), were investigated, but their activity and product N_2 selectivity were lower than those of vanadia catalysts in the presence of H_2O and SO_2 (2).

Recently, H-zeolites and ion-exchanged molecular sieves (e.g., ZSM-5, mordenite, Y-zeolite, pillared clays) have received much attention for the SCR of NO by both hydrocarbon and ammonia (11–21). Wark *et al.* (17) investigated a series of vanadium-containing ZSM-5 catalysts for the ammonia SCR reaction. They found that the activity on the VO^{2+}-exchanged ZSM-5 was higher than that on $(VO_{2.5})_x$–ZSM-5 prepared via chemical vapor deposition of $VOCl_3$. They concluded that isolated VO^{2+} ions were the active sites for the SCR reaction. This is different from vanadia-doped catalysts where V=O and/or V−OH with +5 valent vanadium are considered to be the active sites (1, 2, 10). The maximum activity of VO–ZSM-5 was close to that of a reference V_2O_5/TiO_2 catalyst (17). In our previous work, pillared clays (PILCs) (14), metal oxide-doped PILCs (16),

[1] To whom correspondence should be addressed. E-mail: yang@umich.edu.

0021-9517/00 $35.00

and Fe^{3+}-exchanged PILCs (18) were investigated as catalysts for the SCR reaction. Pillared clays are unique two-dimensional zeolite-like materials. They are prepared by exchanging the charge-compensating cations between the clay layers with larger inorganic hydroxy metal cations followed by dehydration and dehydroxylation at high temperatures. The formed metal oxide clusters (i.e., pillars) keep the silicate layers separated and create interlayer spacing of molecular dimensions. The pillared clays have strong surface acidity and good activities (14). Among the PILC catalysts, $Fe_2O_3 + Cr_2O_3/TiO_2$-PILC and Fe-exchanged TiO_2-PILCs were found to be more active than the commercial $V_2O_5 + WO_3/TiO_2$ catalyst (16, 18). In particular, the SCR activity on the Fe–TiO_2-PILCs was improved by the presence of H_2O and SO_2, which was attributed to an increase in surface acidity due to sulfation of the catalysts (18). It is well known that surface acidity is important for the ammonia SCR reaction because a strong acidity is beneficial for the adsorption and activation of ammonia (1, 2). The surface acid sites on TiO_2-PILC are different from those on TiO_2. Both Brønsted acid sites and Lewis acid sites exist on TiO_2-PILC, while only Lewis acid sites exist on TiO_2 (2, 14, 18, 22). It should be interesting to investigate vanadia-containing TiO_2-PILCs and compare them with V_2O_5/TiO_2 for the SCR reaction. In this paper, we investigated a series of VO^{2+}-exchanged TiO_2-PILC catalysts for the SCR reaction. The catalysts were also characterized by spectroscopy and other techniques. These techniques included surface area measurement, pore size distribution, XRD (X-ray diffraction), XPS (X-ray photoelectron spectroscopy), ESR (electron spin resonance), and *in situ* Fourier transform infrared (FTIR) spectroscopy. The oxidation state and the position of vanadium as well as the interactions between VO–TiO_2-PILC and various gases, e.g., NO, $NO + O_2$, and NH_3, have been studied.

EXPERIMENTAL

Catalyst Preparation

TiO_2-pillared clay was synthesized by following the established procedures (18, 23). The starting clay was a purified montmorillonite, i.e., a purified-grade bentonite powder from Fisher Co., with particles less than or equal to 2 μm. The TiO_2-PILC obtained was a delaminated pillared clay that exhibited no (001) reflection (18). It had the following composition: 39.7% SiO_2, 9.7% Al_2O_3, 1.7% Fe_2O_3, 35.2% TiO_2, 0.2% Na_2O, 1.1% MgO, 0.1% CaO, and 0.2% K_2O. The VO^{2+}-exchanged TiO_2-PILC catalysts were prepared by using the conventional ion-exchange procedure. In each experiment, 2 g TiO_2-PILC was added to 200 ml of 0.02 M $VOSO_4$ solution with constant stirring. Four VO–TiO_2-PILC samples with different vanadium contents were prepared under different ion-exchange conditions. The detailed conditions and the resulting V contents are summarized in Table 1. The mixtures were filtered and washed five times with deionized water. The solid samples obtained were first dried at 120°C in air for 12 h and then calcined at 400°C for 6 h. Finally, the samples obtained were ground to 60–140 mesh. The vanadium contents (obtained by neutron activation analysis) in VO(2)–TiO_2-PILC, VO(3)–TiO_2-PILC, VO(4)–TiO_2-PILC, and VO(13)–TiO_2-PILC were 2.1, 2.5, 3.5, and 13.2 wt%, respectively (Table 1). In addition to pillared clay catalysts, 4.4 wt% $V_2O_5 + 8.2$ wt% WO_3/TiO_2 catalyst was also prepared by incipient wetness impregnation (16) and used for comparison. The $V_2O_5 + WO_3/TiO_2$ catalyst had SCR activity and behavior nearly identical to that of the commercial SCR catalyst made by a major catalyst manufacturer (16).

TABLE 1

Preparation Conditions and Vanadium Contents of the VO–TiO_2-PILC Catalysts

Sample	V content (wt%)	Preparation conditions
VO(2)–TiO_2-PILC	2.1	Ion exchange for 8 h at room temperature (once)
VO(3)–TiO_2-PILC	2.5	Ion exchange for 24 h at room temperature (once)
VO(4)–TiO_2-PILC	3.5	Ion exchange for 24 h at room temperature (3 times)
VO(13)–TiO_2-PILC	13.2	Ion exchange for 24 h at 50°C (3 times)

Catalytic Activity Measurement

The SCR activity measurement was carried out in a fixed-bed quartz reactor. The reaction temperature was controlled by an Omega (CN-2010) programmable temperature controller. In this work, 0.3 g catalyst was used. The flue gas was simulated by blending different gaseous reactants. The typical reactant gas composition was as follows: 1000 ppm NO, 1000 ppm NH_3, 2% O_2, 1000 ppm SO_2 (when used), 8% water vapor (when used), and balance He. The total flow rate was 500 ml/min (ambient conditions) and the GHSV (gas hourly space velocity) was 75,000 h^{-1}. The premixed gases (1.01% NO in He, 1.00% NH_3 in He, and 0.99% SO_2 in He) were supplied by Matheson. Water vapor was generated by passing He through a heated gas-wash bottle containing deionized water. The tubings of the reactor system were wrapped with heating tapes to prevent formation and deposition of ammonium sulfate/bisulfate and ammonium nitrate. The NO and NO_2 concentrations were continually monitored by a chemiluminescent NO/NO_x analyzer (Thermo Electron Corp., Model 10). To avoid errors caused by the oxidation of ammonia in the converter of the NO/NO_x analyzer, an ammonia trap containing

phosphoric acid solution was installed before the sample inlet to the chemiluminescent analyzer. The products were also analyzed by a gas chromatograph (Shimadzu, 14A) with a 5A molecular sieve column for N_2 and a Porapak Q column for N_2O, both at 50°C. All the data were obtained after 10 min when the SCR reaction reached steady state.

Catalyst Characterization

Powder XRD was conducted with a Rigaku Rotaflex D/Max-C system with Cu$K\alpha$ ($\lambda = 0.1543$ nm) radiation. The samples were loaded on a sample holder with a depth of 1 mm. XRD patterns were recorded in the range of $2\theta = 2$–45°.

A Micromeritics ASAP 2010 micropore size analyzer was used to measure the N_2 adsorption isotherms of the samples at liquid N_2 temperature (−196°C). The specific surface areas of the samples were determined from the linear portion of the BET plots ($P/P_0 = 0.05$–0.20). The pore size distribution was calculated from the desorption branch of the N_2 adsorption isotherm using the Barrett–Joyner–Halenda formula, because the desorption branch can provide more information about the degree of blocking than the adsorption branch. Prior to the surface area and pore size distribution measurements, the samples were dehydrated at 350°C for 6 h.

ESR spectra were recorded on a Brucker EMX ESR spectrometer, under the conditions of a microwave power of 6.3 mW and a modulation amplitude of 5.0 G. Before the ESR experiment, TiO_2-PILC and VO–TiO_2-PILC samples were first treated at 300°C in flowing He to remove adsorbed water. The samples were sealed in Pyrex tubes at room temperature under He atmosphere. The sealed samples were then transferred to the ESR sample holder and the ESR spectra were recorded at 20°C.

The XPS experiment was carried out on a Perkin–Elmer PHI 5400 ESCA system at room temperature under 10^{-8}–10^{-9} Torr, using Mg$K\alpha$ radiation. The binding energies for Ti $2p_{3/2}$ and V $2p_{3/2}$ were calibrated relative to the carbon impurity with a C1s band at 284.7 eV.

Infrared spectra were recorded on a Nicolet Impact 400 FTIR spectrometer with a TGS detector. Self-supporting wafers of 1.3-cm diameter were prepared by pressing 30-mg samples and were loaded into a high-temperature IR cell with BaF_2 windows. The wafers were first treated at 450°C in a flow of He (99.9998%, 100 ml/min) for 15 min and then cooled to a desired temperature, i.e., 400, 300, 200, 100, and 30°C. At each temperature, the background spectrum was recorded in He and was subtracted from the sample spectrum that was obtained at the same temperature. Thus the IR absorption features that originated from the structural vibrations of the catalyst were eliminated from the sample spectra. In the experiment, the IR spectra were recorded by accumulating either 100 or 8 scans at a spectral resolution of 4 cm^{-1}. During the FTIR experiments, the gas mixtures (i.e., NO/He, NO + O_2/He, NH_3/He and NO + NH_3 + O_2/He) had the same concentrations as that used in the activity measurements, i.e., 1000 ppm NO (when used), 1000 ppm NH_3 (when used), 2% O_2 (when used), and balance of He. The total gas flow rate was 500 ml/min (ambient conditions).

RESULTS

Catalytic Performance

The catalytic performance of TiO_2-PILC and VO–TiO_2-PILC for ammonia SCR in the absence of H_2O and SO_2 is summarized in Table 2. Pure TiO_2-PILC showed a low

TABLE 2

Catalytic Performance of VO–TiO_2-PILC Catalysts[a]

Catalyst	Temperature (°C)	NO conversion (%)	Selectivity (%) N_2	Selectivity (%) N_2O	k^b (cm^3/g/s)
TiO_2-PILC	200	2.0	100	0	0.89
	250	3.2	100	0	1.6
	300	5.0	100	0	2.7
	350	9.0	100	0	5.5
	375	12.5	100	0	8.06
	400	19.0	100	0	13.2
VO(2)–TiO_2-PILC	200	12.0	100	0	5.64
	250	35.0	100	0	21.0
	300	65.0	100	0	56.1
	350	88.0	100	0	123
	375	93.0	100	0	161
	400	93.0	100	0	167
VO(3)–TiO_2-PILC	200	20.6	100	0	10.2
	250	47.8	100	0	31.7
	300	72.5	100	0	68.9
	350	89.3	100	0	130
	375	93.5	99.8	0.2	165
	400	93.0	99.6	0.4	167
VO(4)–TiO_2-PILC	200	34.3	100	0	18.5
	250	65.4	100	0	51.7
	300	86.0	100	0	105
	350	94.0	99.2	0.8	163
	375	94.5	98.8	1.2	175
	400	93.8	97.7	2.3	174
VO(13)–TiO_2-PILC	200	50.4	99.3	0.7	30.9
	250	65.3	99.0	1.0	51.6
	300	80.0	98.5	1.5	85.9
	350	85.0	97.0	3.0	110
	375	83.5	95.3	4.7	109
	400	70.0	92.3	7.7	75.5
4.4% V_2O_5 + 8.2% WO_3/TiO_2	350	92.2	97.2	2.8	148
	375	93.0	95.3	4.7	161
	400	90.5	91.8	8.2	148

[a] Reaction conditions: 0.3 g catalyst, [NO] = [NH_3] = 1000 ppm, [O_2] = 2%, balance is He, total flow rate is 500 ml/min, and GHSV = 75 000 h^{-1}.
[b] First-order rate constant, as defined in the text, calculated by Eq. [1].

level of activity for NO reduction at 200–400°C. Only 2.0–19.0% NO conversion was obtained at 200–400°C under the conditions of 1000 ppm NO, 1000 ppm NH_3, 2% O_2, and GHSV = 75,000 h^{-1}. When VO^{2+} ions were exchanged to the TiO_2-PILC, the activity was enhanced significantly under the same conditions. NO conversion for the VO–TiO_2-PILC catalysts increased with temperature at first, passing through a maximum at 350 or 375°C and then decreased slightly at higher temperatures. At low temperatures (e.g., 200 and 250°C), the activity increased with an increase in vanadium content. The product selectivity for N_2 was high (>97.7%) on the VO–TiO_2-PILC catalysts with 2.1–3.5 wt% vanadium content at 200–400°C (Table 2). However, for the catalyst with 13.2 wt% vanadium, N_2 selectivity declined rapidly when the temperature was above 350°C; i.e., much N_2O was formed at higher temperatures, due to the oxidation of ammonia by oxygen (1, 2). The oxidation of ammonia by oxygen also resulted in a decrease in NO conversion at high temperatures for VO(13)–TiO_2-PILC. The maximum NO conversion (94.5%) was obtained on VO(4)–TiO_2-PILC at 375°C among these catalysts. The VO–TiO_2-PILC catalysts with 2.1–3.5 wt% vanadium showed NO conversions similar to that of the commercial $V_2O_5 + WO_3/TiO_2$ catalyst under the same conditions (Table 2), but the former had higher product N_2 selectivities.

Since the reaction is known to be first order with respect to NO under stoichiometric NH_3 conditions on vanadia and pillared clay catalysts (1, 2, 24), the SCR activity can also be represented quantitatively by a first-order rate constant (k). By assuming plug flow reactor (in a fixed bed of catalyst) and free of diffusion limitation, the rate constant k can be calculated from the NO conversion (X) by

$$k = -\frac{F_0}{[\mathrm{NO}]_0 W} \ln(1 - X), \qquad [1]$$

where F_0 is the molar NO feed rate, $[NO]_0$ is the molar NO concentration at the inlet (at the reaction temperature), and W is the catalyst amount (g). From the NO conversions and catalyst amounts, first-order rate constants were calculated and are compared in Table 2. The maximum k value (175 $cm^3/g/s$ at 375°C) of VO(4)–TiO_2-PILC was close to that of the commercial $V_2O_5 + WO_3/TiO_2$ (161 $cm^3/g/s$), but lower than that of Fe^{3+}-exchanged TiO_2-PILC (244 $cm^3/g/s$ at 400°C) (18, 26).

The effects of H_2O and SO_2, separately and together, on the SCR activity of VO(4)–TiO_2-PILC were also studied (Fig. 1). When 8% H_2O was added to the reactants, NO conversion decreased at low temperatures. The inhibition by water decreased with increasing temperature. SO_2 and $H_2O + SO_2$ also decreased NO conversion at low temperatures, but the inhibition was negligible when the temperature was above 375°C. The effect of time-on-stream on the SCR activity in the presence of H_2O and SO_2 is shown in Fig. 2. The result showed that the VO(4)–TiO_2-PILC is a

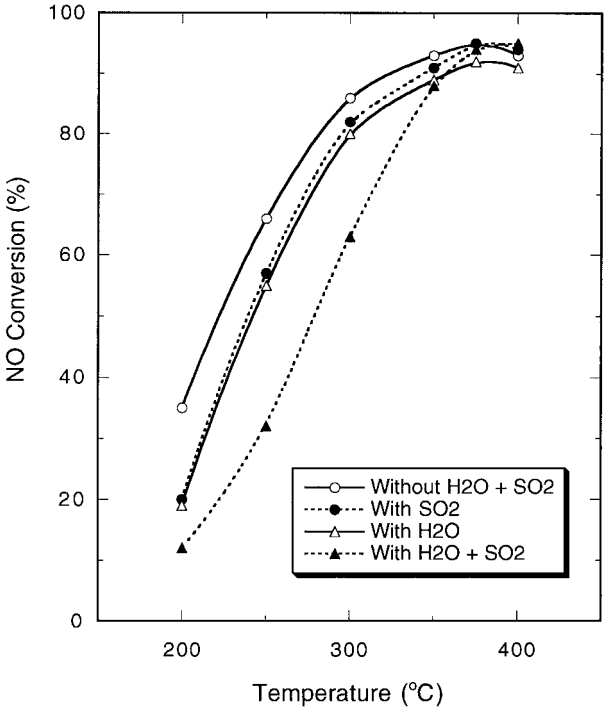

FIG. 1. Effects of H_2O and SO_2 (separately and together) on catalytic activity for VO(4)–TiO_2-PILC (3.5 wt% vanadium) catalyst. Reaction conditions: 0.3 g catalyst, $[NO] = [NH_3] = 1000$ ppm, $[O_2] = 2\%$, $[H_2O] = 8\%$ (when used), $[SO_2] = 1000$ ppm (when used), balance He, total flow rate is 500 ml/min, and GHSV = 75,000 h^{-1}.

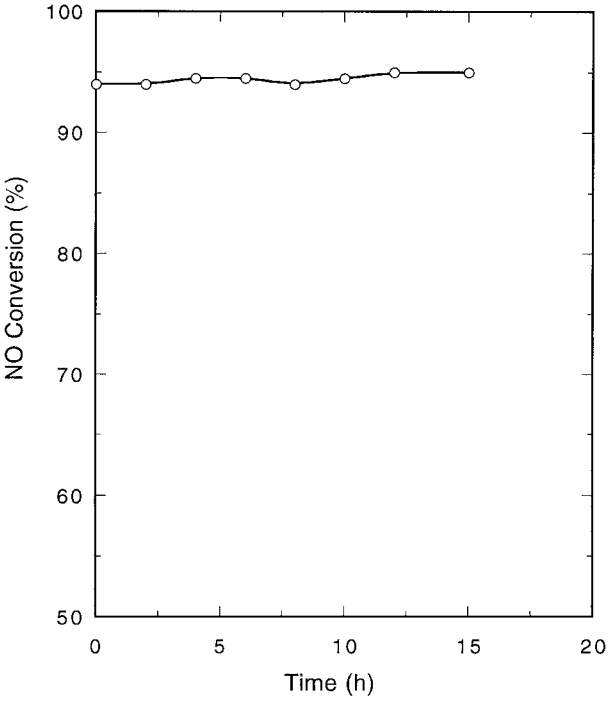

FIG. 2. Effect of time on the VO(4)–TiO_2-PILC in the presence of H_2O and SO_2. Reaction conditions: T = 375°C, 0.3 g catalyst, $[NO] = [NH_3] = 1000$ ppm, $[O_2] = 2\%$, $[H_2O] = 8\%$, $[SO_2] = 1000$ ppm, balance He, total flow rate is 500 ml/min, and GHSV = 75,000 h^{-1}.

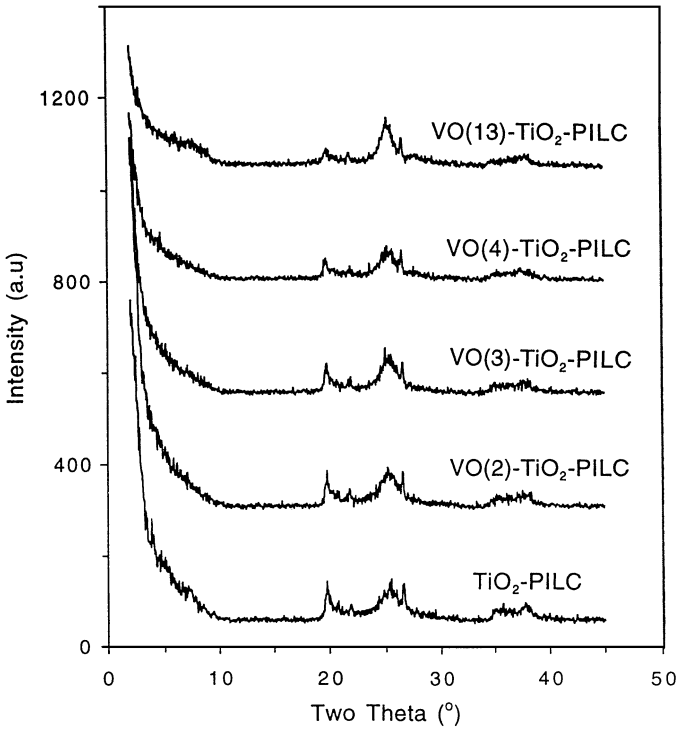

FIG. 3. XRD patterns of TiO_2-PILC and VO–TiO_2-PILC catalysts (the numbers in parentheses denote the approximate wt% of V; see text for details).

stable catalyst for the SCR reaction. During 15 h on stream at 375°C, NO conversion was almost unchanged and the product N_2 selectivity was above 99%.

XRD Analysis

XRD patterns of TiO_2-pillared clay and VO^{2+}-exchanged TiO_2-pillared clays are shown in Fig. 3. The XRD pattern of the TiO_2-PILC showed that it was a delaminated pillared clay that exhibited no (001) reflection (27, 28). The delaminated pillared clays usually show larger pore diameters than laminated pillared clays. The peak at 19.7° is the summation of *hk* indices of (02) and (11) and that at 35.0° is the summation of *hk* indices of (13) and (20) (27, 28). The peaks at 25.3° and 26.5° come from (101) diffractions of anatase TiO_2 and quartz impurities, respectively. The XRD patterns of VO–TiO_2-PILC samples were similar to that of TiO_2-PILC and no peak for vanadium oxides was observed, even when vanadium content reached 13.2 wt% in VO(13)–TiO_2-PILC. This suggested that the particle size of vanadium oxides was smaller than 4 nm and therefore the vanadium oxides were dispersed well on TiO_2-PILC.

Main Characteristics of VO–TiO_2-PILC

The BET surface areas, pore volumes, and pore size distributions of VO–TiO_2-PILC catalysts are summarized in Table 3 and Fig. 4. TiO_2-PILC showed a BET surface area

TABLE 3

Characterization of the Catalysts

Sample	BET surface area (m^2/g)	Pore volume (cm^3/g)	Bimodal pore diameters (nm)
TiO_2–PILC	310	0.32	2.2, 3.7
VO(2)–TiO_2-PILC	292	0.32	2.3, 3.7
VO(3)–TiO_2-PILC	299	0.34	2.4, 3.7
VO(4)–TiO_2-PILC	295	0.31	2.4, 3.7
VO(13)–TiO_2-PILC	172	0.24	2.4, 3.6

of 310 m^2/g, which is much larger than that of unpillared bentonite (30 m^2/g). After a small amount of VO^{2+} ions (<3.5 wt% of vanadium) were exchanged to TiO_2-PILC, the surface area decreased slightly (Table 3). However, for VO(13)–TiO_2-PILC, the surface area decreased sharply to 172 m^2/g. The pore volumes of all the samples were 0.24–0.34 cm^3/g. As shown in Fig. 4, most samples showed a bimodal macropore size distribution, centered at 2.3 and 3.7 nm. With an increase in vanadium content, the macropore volume for the smaller pore (2.3 nm) decreased sharply (Fig. 4), indicating that vanadium oxides blocked some small pores in the pillared clay. The significant decrease in the specific surface area for VO(13)–TiO_2-PILC was likely due to a blockage of small pores by excess vanadium oxides (Fig. 4).

XPS Spectra of VO–TiO_2-PILC

The XPS results of Ti $2p_{3/2}$ and V $2p_{3/2}$ on the fresh TiO_2-PILC and VO–TiO_2-PILC catalysts are summarized in Table 4. A broad XPS band near 459 eV was observed on these samples. This value is almost the same as the binding energy of $2p_{3/2}$ of Ti on TiO_2 (29). Another band centered at 517 eV was detected on the vanadium-containing samples. This value is higher than the V $2p_{3/2}$ binding energy ($\approx$516 eV) for $VOSO_4$, $VOCl_2$, and VO_2, but falls in the range (516.6–517.5 eV) of V_2O_5 (29). This indicates that vanadium on the fresh catalysts was present mainly as the +5 valence form, probably as V_2O_5. Oxygen oxidized

TABLE 4

XPS Data of VO–TiO_2-PILC Catalysts

Sample	Binding energy (eV)		$(V/Ti)_s$[a]	$(V/Ti)_b$[b]
	Ti $2p_{3/2}$	V $2p_{3/2}$		
TiO_2-PILC	459.4	—	0	0
VO(2)–TiO_2-PILC	459.3	517.1	0.21	0.094
VO(4)–TiO_2-PILC	459.3	516.9	0.35	0.15
VO(13)–TiO_2-PILC	459.1	517.3	0.57	0.58

[a] Surface atomic ratio, obtained from XPS spectra.
[b] Bulk atomic ratio, obtained from neutron activation analysis.

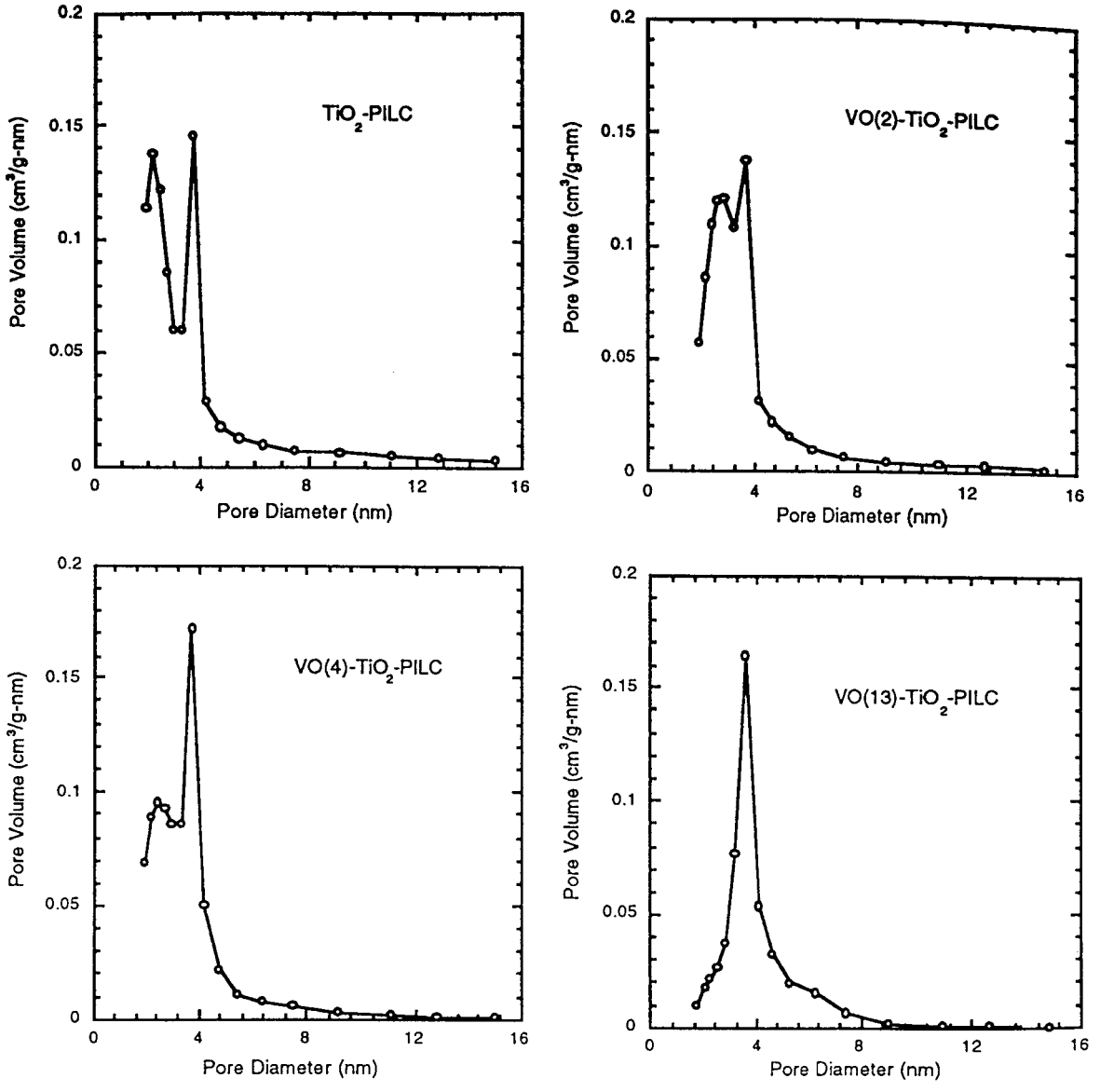

FIG. 4. Pore size distribution for TiO_2-PILC and VO–TiO_2-PILC catalysts.

vanadyl to V_2O_5 during calcination at 400°C in air. As expected, the intensity of the V $2p_{3/2}$ band increased with the vanadium content on the VO–TiO_2-PILC samples. Surface V/Ti ratios were much higher than bulk V/Ti ratios for VO(2)–TiO_2-PILC and VO(4)–TiO_2-PILC, but they were almost the same for VO(13)–TiO_2-PILC. This suggests that V_2O_5 crystals probably existed on the sample with high vanadium content.

ESR Spectra of VO–TiO_2-PILC

The ESR spectra of TiO_2-PILC and VO–TiO_2-PILC catalysts are shown in Fig. 5. After TiO_2-PILC was treated at 300°C for 30 min in He and then cooled to room temperature, a strong narrow line at $g = 4.29$ and a weak signal at $g \approx 2.00$ were detected on the ESR spectrum (Fig. 5). The signal at $g = 4.29$ can be assigned to Fe^{3+} ions in tetrahedral coordination in TiO_2-PILC (30, 31). The weak signal at $g \approx 2.0$ originates from iron oxide. The iron ions and oxide come from the original clay material (i.e., montmorillonite). It is noted that the sample was sealed in a Pyrex tube and the empty Pyrex tube also showed a signal at $g = 4.29$, but the intensity was only one-sixth of that of the TiO_2-PILC. After VO–TiO_2-PILC catalysts were pretreated at 300°C in He, the signals of eight-line hyperfine patterns ($g_\perp \approx 1.99$ and $g_\parallel \approx 1.94$) were observed at 20°C, in addition to a signal at $g = 4.29$. The eight-line hyperfine patterns are the characteristic signals of V(IV) due to the interaction of the unpaired electron with the ^{51}V nucleus ($I = 7/2$) (32, 33). This indicates that vanadyl species existed on the

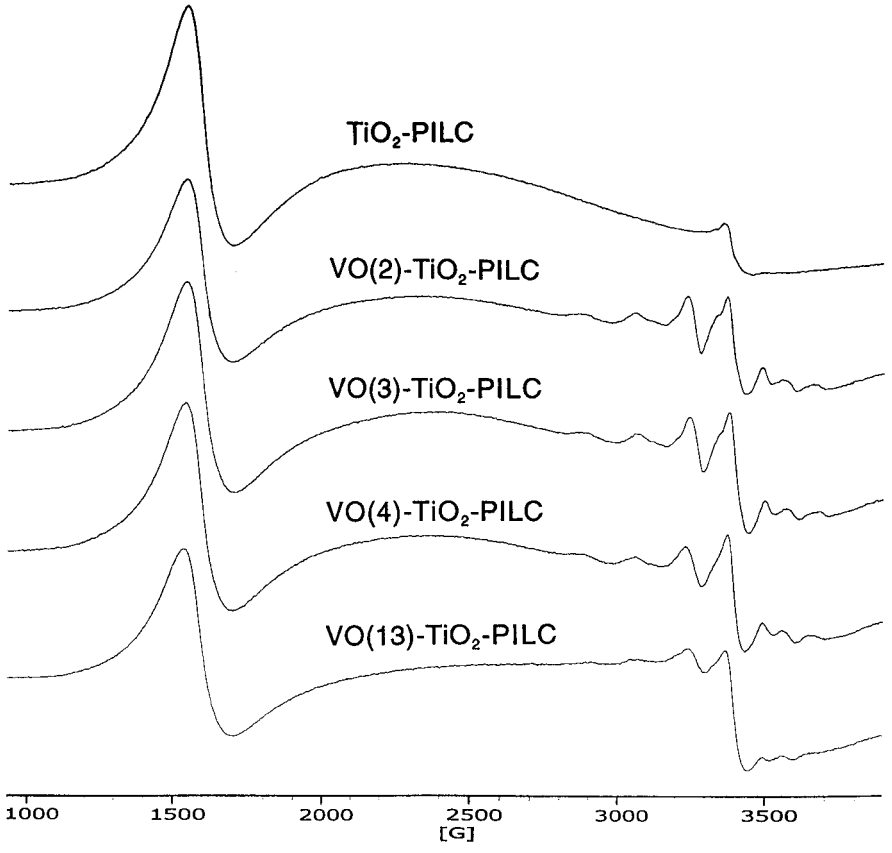

FIG. 5. ESR spectra at 20°C of TiO_2-PILC and VO–TiO_2-PILC catalysts that were pretreated at 300°C in He.

VO–TiO_2-PILC catalysts that were pretreated at 300°C. However, these signals due to the +4 valence vanadium were very weak or could not be observed on the samples that were not pretreated at 300°C in He. This is in accordance with the above XPS results that vanadium on the fresh catalysts was present mainly as V_2O_5, not VO^{2+}.

FTIR Study

Ammonia adsorption on the catalysts was first investigated by FTIR spectroscopy. Prior to ammonia adsorption, the catalysts were treated at 450°C for 15 min in flowing He and then cooled to room temperature. Subsequently, 1000 ppm NH_3/He was passed over the catalysts for 30 min followed by He purge for 15 min. The IR spectra of ammonia adsorbed on TiO_2-PILC and VO–TiO_2-PILC samples at 30°C are shown in Fig. 6. One strong band at 1451 cm^{-1} and three weaker bands at 1670, 1596, and 1242 cm^{-1} were observed on TiO_2-PILC (Fig. 6). The bands at 1670 and 1451 cm^{-1} are assigned to the symmetric and asymmetric bending vibrations of NH_4^+ ions that are chemisorbed on the Brønsted acid sites, while the bands at 1596 and 1242 cm^{-1} can be assigned to the asymmetric and symmetric vibrations of the N–H bonds in NH_3 coordinately linked to the Lewis acid sites (25, 34). It is clear that there are many more Brønsted acid sites than Lewis acid sites on the TiO_2-PILC at room temperature. When vanadyl ions were exchanged to TiO_2-PILC, the intensity of the 1451-cm^{-1} band increased (Fig. 6), indicating more Brønsted acid sites on the surface. Moreover, this band shifted to lower wavenumbers for the VO–TiO_2-PILC catalysts (e.g., 1422 cm^{-1} on VO(13)–TiO_2-PILC). With an increase in vanadium content, the Brønsted acidity increased, but a change in Lewis acidity was not apparent.

Figure 7 shows the IR spectra of NO + O_2/He adsorbed on TiO_2-PILC and VO–TiO_2-PILC catalysts at room temperature. After TiO_2-PILC was treated in flowing 1000 ppm NO + 2% O_2/He for 30 min and then purged with He for 15 min, four intense bands at 1611, 1580, 1291, and 1250 cm^{-1} as well as a weak band at 1490 cm^{-1} were observed (Fig. 7). The bands at 1580, 1490, 1291, and 1250 cm^{-1} can be assigned to nitrate species (24, 35–37). The band at 1611 cm^{-1} is very close to the asymmetric stretching frequency of gaseous NO_2 molecules (1617 cm^{-1}) (35). Our previous work also showed that this species had a different thermal stability from the above nitrate species; i.e., it was more stable at high temperatures (24). It is probably due to an NO_2 adspecies (nitro or adsorbed NO_2 molecules) (24, 36, 37). The above results indicate that in the presence of oxygen, NO on TiO_2-PILC can be oxidized to NO_2 and

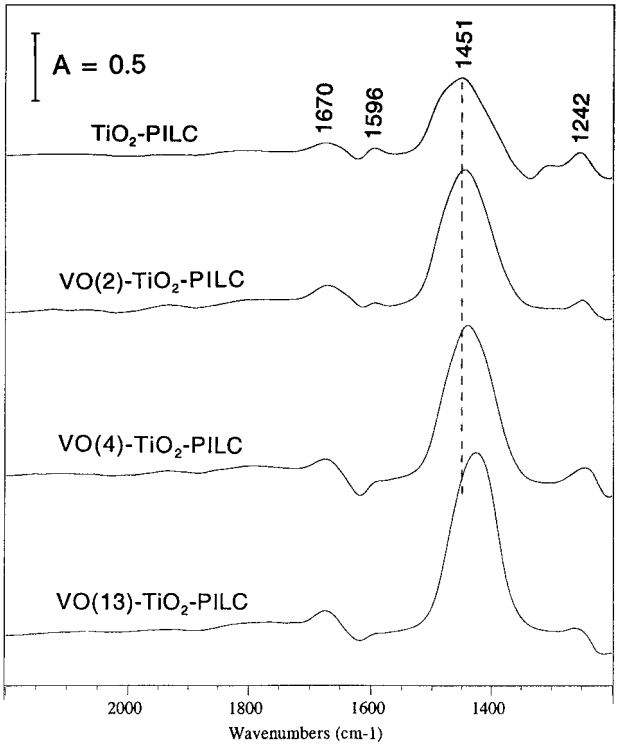

FIG. 6. IR spectra (100 scans) of chemisorbed 1000 ppm NH_3/He at 30°C on TiO_2-PILC and VO–TiO_2-PILC catalysts.

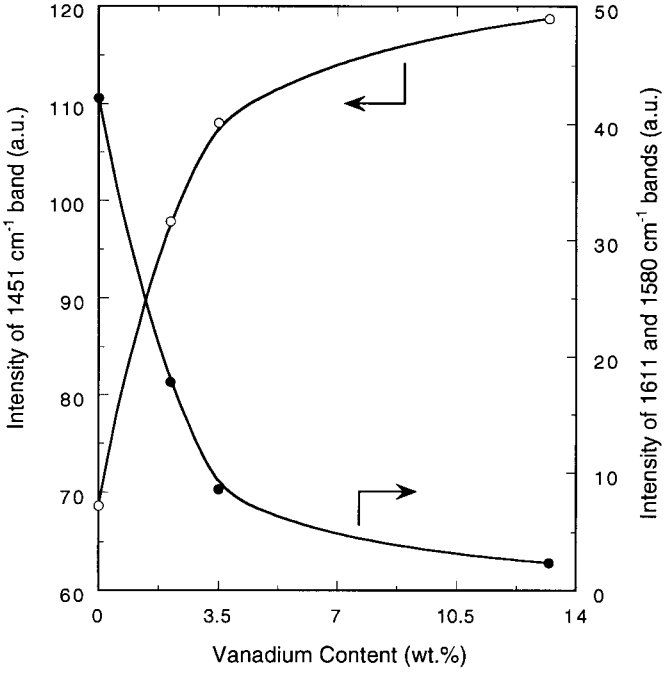

FIG. 8. Dependence on vanadium content of the Brønsted acidity (indicated by band intensity at 1451 cm^{-1} by NH_3 adsorption) and of the NO_x adsorption amount (indicated by band intensity at 1611 and 1580 cm^{-1}) for the TiO_2-PILC and VO–TiO_2-PILC catalysts.

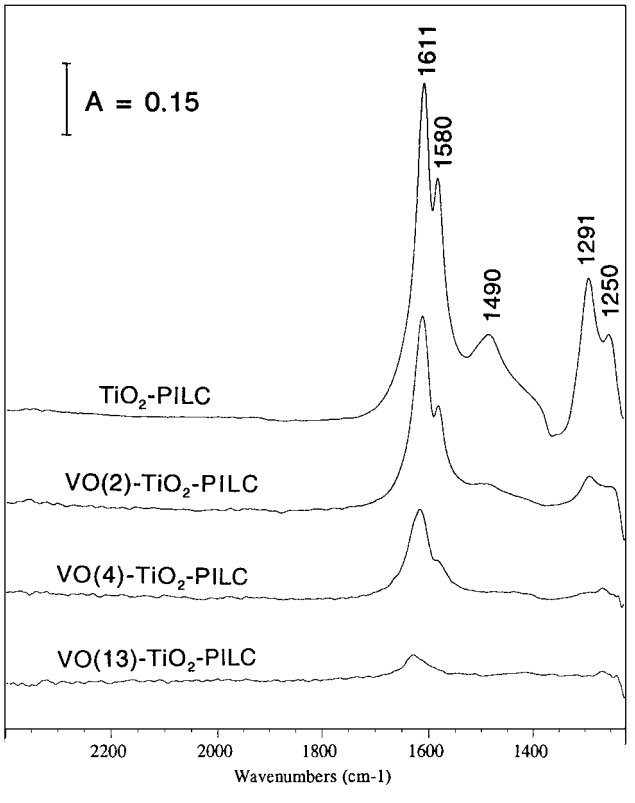

FIG. 7. IR spectra (100 scans) of chemisorbed 1000 ppm NO + 2% O_2/He at 30°C on TiO_2-PILC and VO–TiO_2-PILC catalysts.

nitrate species. The IR bands due to NO_2 and nitrate adspecies were also observed in the spectra of $NO + O_2$ adsorbed on VO–TiO_2- PILC, but their intensities were lower than that on TiO_2-PILC (Fig. 7). This suggests that the addition of vanadium to TiO_2-PILC decreased NO_x adsorption. With increasing vanadium content, the intensities of the IR bands due to NO_x adspecies decreased sharply on the VO–TiO_2-PILC catalysts. Only a very weak band at 1611 cm^{-1} was detected in the spectrum of $NO + O_2$ adsorbed on VO(13)–TiO_2-PILC. The relationships between NH_3 adsorption and NO_x adsorption on VO–TiO_2-PILC catalysts are shown in Fig. 8. The intensities of IR bands at 1451 cm^{-1} and at 1611 and 1580 cm^{-1} are chosen as adsorption amounts for NH_3 and NO_x, respectively, because they are stronger than the other IR bands. It clearly shows that the ammonia adsorption amount (i.e., Brønsted acidity) increased, but the NO_x adsorption amount decreased with increasing vanadium content on the VO–TiO_2-PILC catalysts.

Figure 9 shows the IR spectra of ammonia adsorbed on VO(4)–TiO_2-PILC at room temperature, followed by purge in He at different temperatures. With an increase in temperature, the intensities of the IR bands due to NH_4^+ ions and coordinated ammonia decreased. This indicates that some of ammonia desorbed from the surface and/or was oxidized by the lattice oxygen of the catalyst. It is known that the lattice oxygen of V_2O_5 can oxidize ammonia to N_2 and

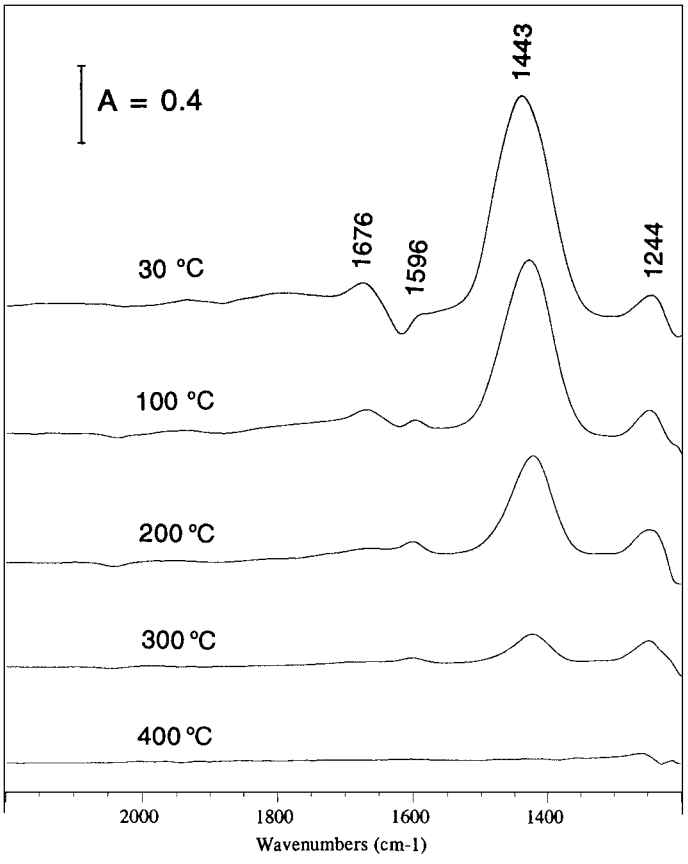

FIG. 9. IR spectra (100 scans) of chemisorbed 1000 ppm NH_3/He on VO(4)–TiO_2-PILC at room temperature followed by purge in He at different temperatures.

nitrogen oxides at high temperatures (38). Upon heating to 400°C, no NH_4^+ or coordinated NH_3 was detected on the surface of VO(4)–TiO_2-PILC. The IR spectra of $NO + O_2$ adsorbed on VO(4)–TiO_2-PILC at different temperatures are shown in Fig. 10. After VO(4)–TiO_2-PILC was treated in $NO + O_2$/He for 30 min and then purged by He for 15 min at room temperature, a strong IR band (1620 cm^{-1}) due to NO_2 adspecies and a shoulder (1582 cm^{-1}) due to nitrate adspecies were observed. With an increase in temperature to 100°C, the band at 1582 cm^{-1} vanished, but the 1620-cm^{-1} band increased slightly (Fig. 10), suggesting that the NO_2 adspecies was more stable than nitrate adspecies on the VO–TiO_2-PILC catalyst. At 300°C, the 1620-cm^{-1} band also disappeared.

Figure 11 shows the reaction at 200°C between ammonia adspecies on VO(4)–TiO_2-PILC and gaseous $NO + O_2$. VO(4)–TiO_2-PILC was first treated with NH_3/He for 30 min followed by He purge for 15 min. $NO + O_2$/He was then introduced into the cell and IR spectra were recorded as a function of time (Fig. 11). As noted above, NH_4^+ ions (1691 and 1425 cm^{-1}) and coordinated NH_3 (1600 and 1259 cm^{-1}) were generated after the VO–TiO_2-PILC was treated with NH_3/He and their IR bands did not decrease in flowing He for 30 min. After $NO + O_2$/He was passed over the sample, the bands attributed to ammonia adspecies decreased with time. After 5 min, the IR bands due to coordinated ammonia vanished, and a new weak band was observed at 1620 cm^{-1} (Fig. 11). This band might come from adsorbed NO_2 or H_2O or both. These results indicate that the reaction between $NO + O_2$ and ammonia adspecies (both NH_4^+ ions and coordinated NH_3) occurred because the IR bands due to ammonia adspecies did not decrease in flowing He. All of the ammonia adspecies bands diminished in 15 min and only a band at 1620 cm^{-1} was detected (Fig. 11). The reactions of NO and O_2, separately, with ammonia adspecies were also studied on VO(4)–TiO_2-PILC (Fig. 12). When 1000 ppm NO was passed over the ammonia adsorbed cata lyst at 200°C, the IR band at 1425 cm^{-1} due to NH_4^+ ions also decreased with time, but the reaction was very slow. After 15 min, only about 25% NH_4^+ ions were consumed by NO (Fig. 12). After 2% O_2 was passed over the ammonia adsorbed sample, the band at 1425 cm^{-1} decreased only slightly in 15 min (Fig. 12).

The reaction between NH_3 and NO_2 adspecies was also studied. In this case, VO(4)–TiO_2-PILC was first treated with $NO + O_2$/He at 200°C for 30 min and then purged

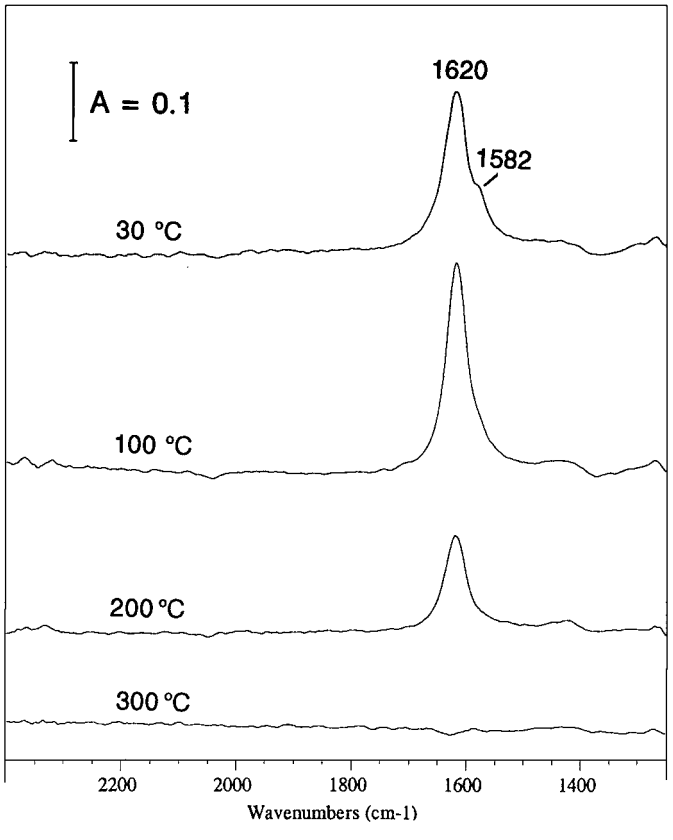

FIG. 10. IR spectra (100 scans) of chemisorbed 1000 ppm NO + 2% O_2/He on VO(4)–TiO_2-PILC at room temperature followed by purge in He at different temperatures.

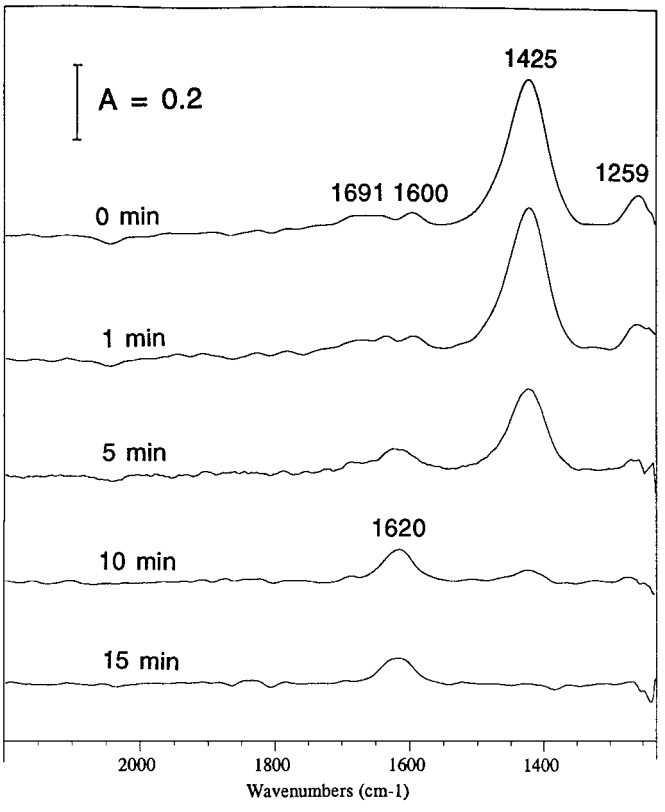

FIG. 11. IR spectra (eight scans) taken at 200°C upon passing 1000 ppm NO + 2% O_2/He over VO(4)–TiO_2-PILC with preadsorbed NH_3.

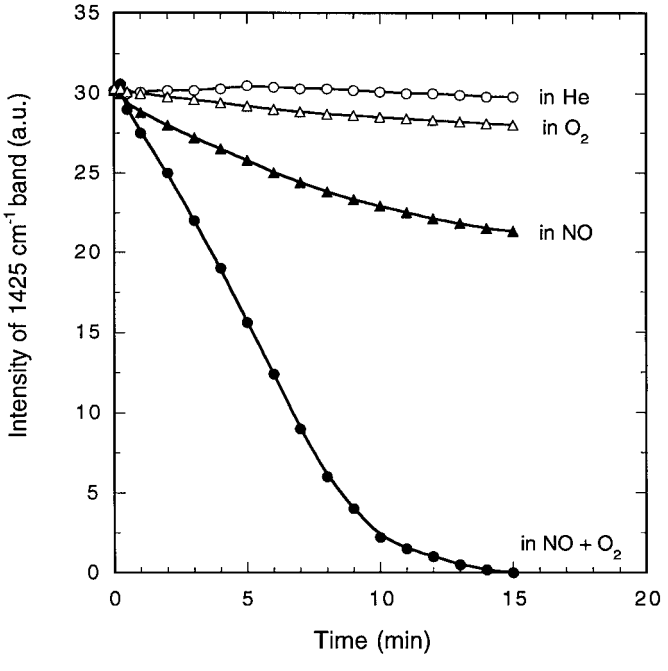

FIG. 12. Consumption of NH_4^+ ions (indicated by band intensity at 1451 cm^{-1}) at 200°C upon passing He, 2% O_2/He 1000 ppm NO/He, and 1000 ppm NO + 2% O_2/He over VO(4)–TiO_2-PILC with preadsorbed NH_3.

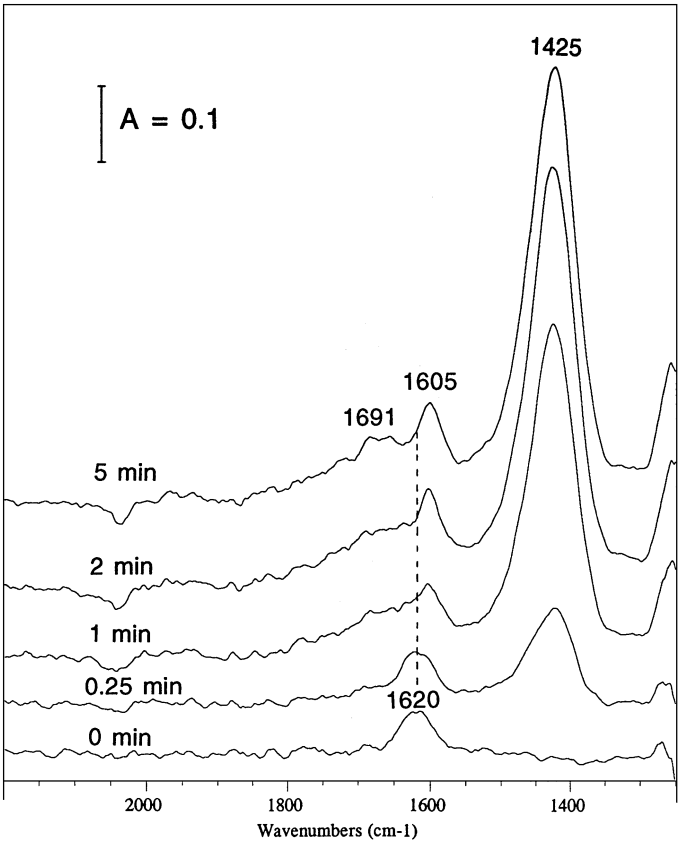

FIG. 13. IR spectra (eight scans) taken at 200°C upon passing 1000 ppm NH_3/He over VO(4)–TiO_2-PILC with preadsorbed NO + O_2.

with He for 15 min. As discussed above, the NO_2 adspecies (1620 cm^{-1}) was observed (Fig. 13). Subsequently, 1000 ppm NH_3/He was passed over the catalyst with preadsorbed NO_2. The IR band at 1620 cm^{-1} decreased in 0.25 min. Meanwhile, IR bands attributed to NH_4^+ ions (1691 and 1425 cm^{-1}) and coordinated NH_3 (1605 cm^{-1}) were formed (Fig. 13). This indicates that the NO_2 adspecies had reacted with ammonia. After 2–5 min, the NO_2 adspecies band almost disappeared and only ammonia adspecies were detected (Fig. 13).

To identify the species present on the catalyst under reaction conditions, IR spectra were recorded for VO(4)–TiO_2-PILC that was heated from 100 to 400°C in a flow of NO + NH_3 + O_2/He. As shown in Fig. 14, the bands due to NH_4^+ ions and coordinated NH_3 species were observed at 1672, 1598, 1434, and 1249 cm^{-1}. An increase in temperature resulted in a decrease in the intensity of the IR bands that were due to NH_4^+ ions and coordinated NH_3 species. All of the IR bands due to ammonia adspecies vanished at 400°C (Fig. 14). Throughout the entire temperature range, no IR bands due to NO_x adspecies were detected in flowing NO + NH_3 + O_2/He, suggesting that the adsorption of NH_3 was much stronger than that of NO_x under the reaction conditions.

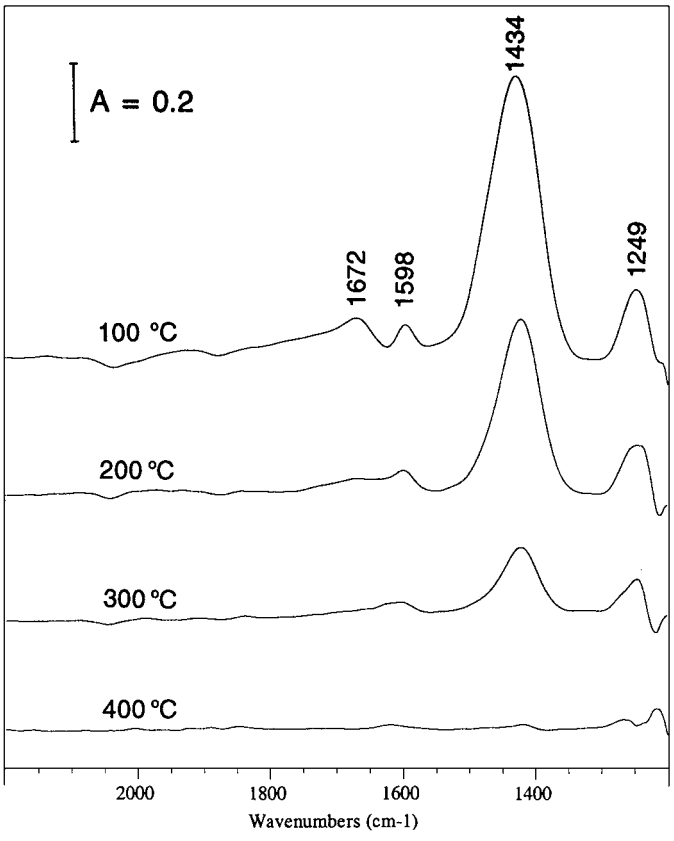

FIG. 14. IR spectra (100 scans) of VO(4)–TiO_2-PILC in a flow of 1000 ppm NO + 1000 ppm NH_3 + 2% O_2/He at 100–400°C.

DISCUSSION

The present results indicated that VO-exchanged TiO_2-PILC catalysts were highly active for ammonia SCR reaction (Table 2). The activity on VO–TiO_2-PILC was much higher (about 13 times) than that of TiO_2-PILC, suggesting that vanadium played an important role in this reaction. In the low temperature range (e.g., 200°C), the SCR activity increased with increasing vanadium content. However, at higher temperatures, an excess vanadium on VO(13)–TiO_2-PILC catalyst resulted in a decrease in NO conversion and also N_2 product selectivity, due to oxidation of ammonia by oxygen. The maximum activity was obtained with 2.1–3.5 wt% vanadium. The VO–TiO_2-PILC catalysts were also resistant to water vapor and sulfur dioxide at high temperatures (>350°C) (Fig. 1). The time-on-stream (at 375°C for 15 h) result indicated that VO–TiO_2-PILC was stable in the presence of $H_2O + SO_2$ (Fig. 2). The maximum SCR activity on the VO–TiO_2-PILC catalysts was almost the same as that on vanadia-doped TiO_2-PILC and commercial $V_2O_5 + WO_3/TiO_2$ catalysts, but higher than that on V_2O_5/TiO_2 (25).

During the process of catalyst preparation, VO^{2+} ions could exchange with cations in TiO_2-PILC, i.e., mainly H^+ and also Na^+, K^+, and Mg^{2+}. After calcination at 400°C in air, most of the VO^{2+} ions were oxidized to V_2O_5 by oxygen, as indicated by the XPS results (Table 4). ESR spectra also showed that the signals due to +4 valent vanadium were very weak or could not be observed on the fresh samples. This is different from VO^{2+}-exchanged ZSM-5 catalysts in which VO^{2+} ions were the dominating species, reported by Wark *et al.* (17). It is known that pillared clay and ZSM-5 have different structures. Isolated VO^{2+} ions in ZSM-5 may not be easily oxidized to V_2O_5. The V_2O_5 formed on the VO–TiO_2-PILC would block some of the smaller pores, as evidenced by the pore size distribution data (Fig. 4). For VO(13)–TiO_2-PILC, the ion-exchange process was carried out at 50°C. Under that condition, some VO^{2+} ions would be hydrolyzed to vanadium hydroxide and precipitated on the surface of TiO_2-PILC. This led to a much higher vanadium content on this sample. After VO–TiO_2-PILC catalysts were heated at 300°C in He, some V_2O_5 was automatically reduced to VO^{2+}, which was identified by the ESR spectra where the signals of the eight-line hyperfine patterns due to VO^{2+} ions were observed on the pretreated samples (Fig. 5). This is in agreement with the earlier finding observed on V_2O_5/TiO_2 (32, 39). Bond *et al.* reported that a few percent of VO^{2+} ions were present on the V_2O_5/TiO_2 that was calcined at 450°C (39). It seems that a redox equilibrium between +4 and +5 valent vanadium exists on the VO–TiO_2-PILC catalysts during the SCR reaction.

It is known that surface acidity is important for ammonia SCR reaction (1, 2). Both Brønsted acid sites and Lewis acid sites exist on TiO_2-PILC and VO–TiO_2-PILC catalysts, with a larger proportion being Brønsted acid sites at room temperature. When ammonia was adsorbed on these samples, NH_4^+ ions and coordinated NH_3 were formed, as shown by IR spectra (Fig. 6). Pillars are the major sources for Lewis acidity on pillared clays (40, 41). It is known that Lewis acid sites exist on the surface of TiO_2 (2). Two sources for Brønsted acidity in pillared clays have been discussed in the literature. One derives from the structural hydroxyl groups in the clay layer (41). The most likely proton site for some smectites (e.g., montmorillonite) is located at the Al(VI)−O−MgO linkage, where Al(VI) is the octahedrally coordinated Al and Mg has replaced an Al in the octahedral layer. Another source of proton derives from the cationic oligomers that upon heating decompose into metal oxide pillars and liberate protons. When VO^{2+} ions were exchanged to TiO_2-PILC, the IR band at 1451 cm^{-1} due to NH_4^+ ions became stronger and also shifted to lower wavenumbers. This suggests that new Brønsted acid sites were created due to the addition of vanadium, although some H^+ ions in the pillared clay were replaced by VO^{2+} ions. Brønsted acid sites are known to be present on the surface of V_2O_5. It was reported that when V_2O_5 was doped on TiO_2, Brønsted acidity was increased significantly (2). The Brønsted acid sites on V_2O_5/TiO_2 were found to be

associated with V^{+5}–OH (42). A treatment in H_2 at 352°C would remove all of the Brønsted acid sites from V_2O_5/TiO_2 due to reduction of vanadia (42). The generation of new Brønsted acid sites on the VO–TiO_2-PILC catalysts further supported the above conclusion that vanadium was present mainly as the +5 valent form. For the VO–TiO_2-PILC catalysts, the Brønsted acidity increased with an increase in vanadium content (Figs. 6 and 8). Furthermore, the position of the NH_4^+ band was also seen to vary with vanadium content; i.e., the more vanadium, the lower are the wavenumbers (Fig. 6). The difference in wavenumbers reflected the presence of the weaker N–H bonds in NH_4^+ ions for the higher vanadium content catalysts. The increase in Brønsted acidity and decrease in wavenumbers for the NH_4^+ band are consistent with the increase in the SCR activity at low temperatures (e.g., 200°C) (Table 2). With increasing temperature, the ammonia adspecies desorbed from the catalyst, but they were still detected at 300°C (Fig. 9). The ammonia adspecies were reactive in reacting with NO and $NO + O_2$ (Figs. 11 and 12). After $NO + O_2$/He were passed over the ammonia that was adsorbed on VO(4)–TiO_2-PILC at 200°C, both NH_4^+ ions and coordinated NH_3 vanished in 5–15 min. By comparison, the reaction between NO and ammonia adspecies was much slower. Only 25% NH_4^+ ions were consumed by NO in 15 min (Fig. 12). It is clear that oxygen had a significant promoting role for this reaction.

The IR spectra showed that $NO + O_2$ could also adsorb on TiO_2-PILC and VO–TiO_2-PILC catalysts, forming NO_2 and nitrate adspecies at room temperature (Fig. 7). The NO_2 adspecies was the dominant species on the catalysts at high temperatures (Fig. 10). With increasing vanadium content, the intensities of the IR bands due to NO_2 and nitrate adspecies decreased significantly (Figs. 7 and 8). Very weak NO_2 bands were observed on the catalyst with high vanadium contents. This is different from Fe^{3+}-exchanged TiO_2- PILC catalysts (24). In that case, the addition of Fe^{3+} ions to TiO_2-PILC enhanced the formation of NO_2. The decrease in NO_x adsorption with vanadium content is not in line with the increase in SCR activity at low temperatures for the VO–TiO_2-PILC catalysts. It is known that NO_x species can adsorb on a titania surface (2, 43), but do not adsorb on an oxidized vanadia surface (2). The above result indicates that V_2O_5 was anchored directly on the surface of titania pillars. With the coverage of titania pillars by V_2O_5, NO_x adsorption became weaker (Fig. 8). Increasing temperature resulted in desorption of NO_x from the VO–TiO_2-PILC (Fig. 10). After NH_3/He was passed over the VO–TiO_2-PILC preadsorbed with NO_x at 200°C, NO_2 adspecies disappeared in 2–5 min (Fig. 13), indicating that NO_2 adspecies were reduced by NH_3.

The foregoing results indicated that both NO_x and NH_3 could be separately adsorbed on VO–TiO_2-PILC catalysts. However, under the SCR reaction conditions, the surface of VO–TiO_2-PILC was found to be covered mainly by NH_4^+ ions and coordinated NH_3 (Fig. 14). No NO_x adspecies was detected. The IR spectra were very similar to that of NH_3 adsorption on VO–TiO_2-PILC (Fig. 9). This indicates that ammonia adsorption was much stronger than NO_x adsorption under the reaction conditions. In combination with the result that SCR activity was in inverse proportion to NO_x adsorption, NO adsorption and oxidation may not play an important role for the SCR reaction on the VO–TiO_2-PILC catalysts. In fact, the reaction rate of NO oxidation to NO_2 by oxygen on the catalysts should be very low. Our previous work showed that, even on TiO_2-PILC, which showed the strongest IR bands of NO_x adspecies in this work, less than 2% NO was oxidized to NO_2 at 250–450°C under the conditions of 1000 ppm NO, 2% O_2, and GHSV $= 1.13 \times 10^5$ h^{-1} (24). This is far below the SCR activity. Therefore, NO molecules may take part in the SCR reaction mainly as gaseous or weakly adsorbed forms for the VO–TiO_2-PILC catalysts. In the SCR reaction, ammonia molecules are first adsorbed on the Brønsted and Lewis acid sites to form NH_4^+ and coordinated NH_3, and then gaseous or weakly adsorbed NO molecules react with these ammonia adspecies to generate N_2 and H_2O. Meanwhile, +5 valent vanadium was reduced to the +4 valent form. The role of oxygen is to oxidize the reduced vanadium back to the +5 valent form. This is different from the mechanism obtained on Fe-exchanged TiO_2-PILC in which NO_2 is an intermediate for the SCR reaction (24), but similar to that on vanadia-doped TiO_2 catalysts (1–10). The major difference in surface acidity between TiO_2-PILC and TiO_2 is that there are more Brønsted acid sites than Lewis acid sites on TiO_2-PILC but no Brønsted acid sites were found on TiO_2. Hence, it is likely that there are more Brønsted acid sites on VO–TiO_2-PILC than on V_2O_5/TiO_2. As a result, VO–TiO_2-PILC showed better SCR activity than V_2O_5/TiO_2 at high temperatures (e.g., 400°C) (25).

CONCLUSIONS

VO-exchanged TiO_2-PILC catalysts were highly active for the reduction of NO by ammonia in the presence of oxygen. These catalysts were also resistant to H_2O and SO_2 at high temperatures. The catalysts showed the same activity as the commercial $V_2O_5 + WO_3/TiO_2$ catalyst. XRD, ESR, XPS, and FTIR results indicated that vanadium was dispersed well on TiO_2 pillars and was present mainly as V_2O_5 on the VO–TiO_2-PILC catalysts. FTIR spectra showed that NH_3 molecules could adsorb on the Brønsted acid and Lewis acid sites on the VO–TiO_2-PILC catalyst to generate, respectively, NH_4^+ ions and coordinated NH_3 species. These NH_3 adspecies were active in reacting with NO and $NO + O_2$. The increase in the Brønsted acidity with vanadium content was consistent with the increase in SCR activity at low temperatures. By comparison, the adsorption

of NO_x on the catalysts was very weak, especially under the reaction conditions. The reaction path for NO reduction by NH_3 on VO–TiO_2-PILC is similar to that on V_2O_5/TiO_2 catalyst; i.e., N_2 originates mainly from the reaction between gaseous or weakly adsorbed NO and NH_3 adspecies.

ACKNOWLEDGMENT

This work was supported by the Electric Power Research Institute.

REFERENCES

1. Bosch, H., and Janssen, F., *Catal. Today* **2**, 369 (1988).
2. Busca, G., Lietti, L., Ramis, G., and Berti, F., *Appl. Catal. B* **18**, 1 (1998).
3. Miyamoto, A., Kobayashi, K., Inomata, M., and Murakami, Y., *J. Phys. Chem*. **86**, 2945 (1982).
4. Janssen, F. J. J. G., van den Kerkhof, F. M. G., Bosch, H., and Ross, J. R. H., *J. Phys. Chem*. **91**, 5921 (1987).
5. Ramis, G., Busca, G., Bregani, F., and Forzatti, P., *Appl. Catal.* **64**, 259 (1990).
6. Chen, J. P., and Yang, R. T., *J. Catal.* **125**, 411 (1990).
7. Went, G. T., Leu, L. J., Rosin, R. R., and Bell, A. T., *J. Catal.* **134**, 492 (1992).
8. Ozkan, U. S., Cai, Y., and Kumthekar, M. W., *J. Catal.* **149**, 390 (1994).
9. Odenbrand, C. U. I., Bahamonde, A., Avila, P., and Blanco, J., *Appl. Catal. B* **5**, 117 (1994).
10. Topsøe, N.-Y., Dumesic, J. A., and Topsøe, H., *J. Catal.* **151**, 241 (1995).
11. Amiridis, M. D., Zhang, T., and Farrauto, R. J., *Appl. Catal. B* **10**, 203 (1996).
12. Nam, I. S., Eldridge, J. W., and Kittrell, J. R., *Stud. Surf. Sci. Catal.* **38**, 589 (1988).
13. Brandin, J. G. M., Andersson, L. A. H., and Odenbrand, C. U., *Catal. Today* **4**, 187 (1989).
14. Yang, R. T., Chen, J. P., Kikkinides, E. S., Cheng, L. S., and Cichanowicz, J. E., *Ind. Eng. Chem. Res.* **31**, 1440 (1992).
15. Sullivan, J. A., Cunningham, J., Morris, M. A., and Keneavey, K., *Appl. Catal. B* **7**, 137 (1995).
16. Cheng, L. S., Yang, R. T., and Chen, N., *J. Catal.* **164**, 70 (1996).
17. Wark, M., Brückner, Liese, T., and Gürnert, E., *J. Catal.* **175**, 48 (1998).
18. Long, R. Q., and Yang, R. T., *J. Catal.* **186**, 254 (1999).
19. Kieger, S., Delahay, G., Coq, B., and Neveu, B., *J. Catal.* **183**, 267 (1999).
20. Long, R. Q., and Yang, R. T., *J. Am. Chem. Soc.* **121**, 5595 (1999).
21. Long, R. Q., and Yang, R. T., *J. Catal.* **188**, 332 (1999).
22. Busca, G., Saussey, H., Saur, O., Lavalley, J. C., and Lorenselli, V., *Appl. Catal.* **14**, 245 (1985).
23. Sterte, J., *Clays Clay Miner.* **34**, 658 (1986).
24. Long, R. Q., and Yang, R. T., *J. Catal.* **190**, 22 (2000).
25. Long, R. Q., and Yang, R. T., *Appl. Catal. B* **24**, 13 (2000).
26. Long, R. Q., and Yang, R. T., *Catal. Lett.* **59**, 39 (1999).
27. Bailey, S. W., *in* "Structures of Clay Minerals and Their X-Ray Indentification" (G. W. Brindley and G. Brown, Eds.), Mineralogical Society Monograph, Vol. 5. pp. 1–123. Mineralogical Society, London, 1980.
28. Pinnavaia, T. J., Tzou, M. S., Landau, S. D., and Raythatha, R., *J. Mol. Catal.* **27**, 195 (1984).
29. Wagner, C. D., Riggs, W. M., Davis, L. E., Moulder, J. F., and Mullenberg, G. E. (Eds.) "Handbook of X-Ray Photoelectron Spectroscopy," Perkin–Elmer, Eden Prairie, 1979.
30. Kucherov, A. V., Montreuil, C. N., Kucherova, T. N., and Shelef, M., *Catal. Lett.* **56**, 173 (1998).
31. Goldfarb, D., Bernardo, M., Strohmaier, K. G., Vaughan, D. E. W., and Thomann, H., *J. Am. Chem. Soc.* **116**, 6344 (1994).
32. Bond, G. C., and Tahir, S. F., *Appl. Catal.* **71**, 1 (1991).
33. Bahranowski, K., Janas, J., Machej, T., Serwicka, E. M., and Vartikian, L. A., *Clay Miner.* **32**, 665 (1997).
34. Topsøe, N. Y., *J. Catal.* **128**, 499 (1991).
35. Laane, J., and Ohlsen, J. R., *Progr. Inorg. Chem*. **27**, 465 (1980).
36. Li, Y., and Armor, J. N., *J. Catal.* **150**, 388 (1994).
37. Chen, H.-Y., Voskoboinikov, T., and Sachtler, W. M. H., *J. Catal.* **180**, 171 (1998).
38. Kosaki, Y., Miyamoto, A., and Murakami, Y., *Bull. Chem. Soc. Jpn.* **52**, 617 (1979).
39. Bond, G. C., Sarkany, J., and Parfitt, G. D., *J. Catal.* **57**, 476 (1979).
40. Burch, R., *Catal. Today* **2**, 185 (1988).
41. He, M. Y., Liu, Z., and Min, E., *Catal. Today* **2**, 321 (1988).
42. Topsøe, N.-Y., Topsøe, H., and Dumesic, J. A., *J. Catal.* **151**, 226 (1995).
43. Yang, R. T., Li, W. B., and Chen, N., *Appl. Catal. A* **169**, 215 (1998).